Hydrogels with Gigantic Thermopower for Low-grade Heat Harvesting

Kuan Sun (kuan.sun@cqu.edu.cn)
Chongqing University https://orcid.org/0000-0002-6391-5270
Yongjie He
Chongqing University
Qi Zhang
Chongqing University
Hanlin Cheng
National University of Singapore
Yang Liu
Chongqing University
Yue Shu
Chongqing University
Yang Geng
Chongqing University
Yujie Zheng
Chongqing University
Bo Qin
Chongqing University
Yongli Zhou
Chongqing University
Shanshan Chen
Chongqing University
Jing Li
Chongqing University
Meng Li
Chongqing University
George Omololu Odunmbaku
Chongqing University
Jianyong Ouyang
National University of Singapore https://orcid.org/0000-0001-9901-0177

Physical Sciences - Article

Keywords: i-TE hydrogels, low-grade thermal energy harvesting, PVA/CsI hydrogel

Posted Date: August 4th, 2021

DOI: https://doi.org/10.21203/rs.3.rs-733328/v1

Abstract

Harvesting energy from the environment to power the self-sustained systems has long been desired1,2. Ionic thermoelectric (i-TE) material with mobile ions as charge carriers has the advantage to generate large thermal voltages at low operating temperatures3-5. Recent works improved the thermopower substantially by modifying the polymer matrix of the i-TE hydrogels6-9. But the mobile ions have not been systematically studied in the context of i-TE hydrogels. This study highlights the role of ions in i-TE hydrogels employing a polyvinyl alcohol (PVA) polymer matrix and a number of ion providers, e.g. KOH, KNO3, KCl, KBr, NaI, KI, and CsI. The relationship between the intrinsic physical parameters of the ion and the thermoelectric performance is established, indicating electronegativity of the cation and the ability to influence the hydrogen bond by the anion are two crucial factors. Among these i-TE hydrogels, PVA/CsI hydrogel exhibits the largest ionic Seebeck coefficient, reaching 52.9 mV K-1, which is the greatest of all i-TE materials reported till date. In addition, PVA/NaI hydrogel exhibits excellent TE properties, with a record ZT value of 5.09 at room temperature. This flexible, inexpensive hydrogel that compatible with large-scale manufacturing shows great promise for low-grade thermal energy harvesting.

Main Text

The conversion of abundant low-grade thermal energy into useful electrical energy is essential for sustainable society development. Thermoelectric (TE) materials can convert waste heat generated by industry, fossil fuels, sunlight and even the human body directly into electricity with no moving parts[2,10,11]. Organic thermoelectric materials exhibit excellent thermoelectric properties near room temperature. This makes them ideal for low-grade heat recovery and for providing power to the devices on the internet of things (IoT)[12–14]. But these devices often require a relatively high voltage (> 1.5 V) and power density[15]. So, improving the thermopower, also known as Seebeck coefficient (*S*), and figure of merit (ZT) of TE materials is crucial for such applications. Furthermore, compared to traditional electronic TE materials, ionic thermoelectric (i-TE) materials exhibit superior thermoelectric and mechanical properties[16–18]. i-TEs are typically based on polymers that can be fabricated into ion conductors[19,20], especially ionic gels[5,21].

The working principle of i-TE materials is based on the Soret effect, whereby a temperature gradient induces an inhomogeneous distribution of cations and anions, resulting in a voltage difference. Electrostatic induction between the ions and electrons in the electrode enables charge storage and release to a load in an external circuit. Thus, it is regarded as a thermionic capacitor[3,22,23]. Previous reports focused on the role of polymer matrix in obtaining large thermopower, also known as Seebeck coefficient[7,24,25]. For example, the Seebeck coefficient of NaOH aqueous solution is less than 1 mV K^{-1}, but it can reach up to 11 mV K^{-1} when incorporated into polyethylene oxide (PEO)[3]. Furthermore, the Seebeck coefficient can vary from − 4 to + 14 mV K^{-1} through changing the interaction strength between poly(vinylidene fluoride-co-hexafluoropropylene) (PVDF-HFP) and the 1-ethyl-3-methylimidazolium bis(trifluoromethylsulfonyl)imide (EMIM:TFSI) ionic liquid depending on PEO content[6]. Furthermore, modified cellulose containing charged nanochannels generates a Seebeck coefficient of 24 mV K^{-1} [7]. Similar strategy has also been applied to quasi-solid ionic gels[26,27]. For example, through the dipole moment interaction between PVDF-HFP and an ionic liquid 1-ethyl-3-methylimidazolium dicyanamide (EMIM:DCA), the thermal voltage reaches 26.1 mV K^{-1} [8]. At present, the record Seebeck coefficient for all reported i-TE materials is 34.5 mV K^{-1}, achieved through a combination of waterborne polyurethane and EMIM:DCA[28]. The examples provided clearly demonstrates the dependency of Seebeck coefficient on polymer type, and its surface properties which dictate its interaction with ions. However, whether the thermopower can be enhanced via manipulating the intrinsic physical properties of ions remains to be demonstrated.

In this work, the properties of cations and anions are investigated separately in the context of ionic thermoelectrics. A series of inorganic compounds including KOH, KNO_3, KCl, KBr, KI, NaI or CsI, is incorporated into polyvinyl alcohol (PVA)

 t Seebeck coefficient changes with the structure breaking

strength of the anions. By comparing the three iodides, the cation with smaller electronegativity and smaller binding energy with the hydroxyl groups on PVA shows greater Seebeck coefficient. After optimization, the PVA/CsI hydrogel exhibits a record Seebeck coefficient of 52.9 mV K^{-1}. Furthermore, an extremely high thermoelectric figure of merit (ZT) of 5.09 is obtained in the PVA/NaI hydrogels, which is more than three times the present ZT record. In addition to the excellent TE performance, our ionic hydrogels also have the advantages of facile preparation, low cost and mechanical robustness. These features together suggest hydrogels containing properly selected ions have great potential for low-grade heat harvesting.

For potassium compounds incorporated into the PVA hydrogel, the Seebeck coefficient changes from 17.7 mV K^{-1} in PVA/KOH hydrogel to 49 mV K^{-1} in PVA/KI hydrogel (Fig. 1a), while the ionic conductivities of these hydrogels are comparable (Supplementary Fig. 1). By comparing the hydrogels containing the three iodides, we found the Seebeck coefficient exhibited a trend, i.e. NaI < KI < CsI. Notably, the Seebeck coefficient of PVA/CsI hydrogel at 0.1 M reaches as high as 52.9 mV K^{-1} (Fig. 1a and Supplementary Fig. 2a). To the best of our knowledge, this is the highest Seebeck coefficient reported for ionic thermoelectric materials till date (Fig. 1b). The result is highly reproducible (see Note 1 in Supplementary Information).

Figures 1c-e and Supplementary Fig. 4 show the thermoelectric properties of the modified PVA hydrogel as a function of CsI, KI or NaI concentration. The maximum Seebeck coefficient in all cases occur at a concentration of about 0.1 M (Fig. 1c, and Supplementary Fig. 4a). This trend is analogous to that observed in electronic thermoelectric materials[29]. However, note that ionic conductivity exhibits a monotonous increase with increasing salt concentration in all three hydrogels (Fig. 1d, and Supplementary Fig. 4b).

However, PVA/NaI hydrogel at a concentration of 1 M exhibits the best PF of 9.47 mW m^{-1} K^{-2}, due to its large ionic conductivity (51.8 mS cm^{-1}) and a Seebeck coefficient of 42.8 mV K^{-1}. The PVA/NaI hydrogel shows a low thermal conductivity of 0.543 W m^{-1} K^{-1} (Supplementary Fig. 5b), yielding a record ionic ZT value of 5.09. This ionic ZT value is more than three times the previous ZT record[26] for ionic conductors in literature (Fig. 1f).

In order to understand the role of the ions, we have conducted a systematic investigation on our i-TE system. First, potentially influencing factors such as electrode type for Seebeck measurement, water evaporation effects, and changing valence states of mobile ions are excluded (see Note 2 in S Supplementary Information). Afterwards, density functional theory (DFT) calculations were employed to reveal the cations effect on Seebeck coefficient. The binding energy of the cations towards PVA, from DFT calculations show a similar trend with their electronegativity (Fig. 2a). Thus, Cs^+ which is furthest from the nearest oxygen atom on PVA (Supplementary Fig. 11) and less bound by hydroxyl groups on PVA, can migrate most rapidly within the hydrogel and thus produces the highest Seebeck coefficient.

Figure 2b shows a digital picture of the PVA hydrogels in inverted vials incorporated with five different potassium compounds. There is a difference in the fluidity in these samples. The PVA/KI hydrogel is on the verge of collapse and it has the best fluidity, followed by PVA/KBr, PVA/KCl and PVA/NO_3; while PVA/KOH has the poorest fluidity. The is also reflected by morphological changes at the micro scale. Scanning electron microscopic (SEM) images (Supplementary Fig. 12) indicate the pristine PVA hydrogel and PVA/KOH sample exhibit a rough surface, implying a strong inter-molecular interaction among polymer chains. In contrast, when potassium halide or KNO_3 is added, the surface of the hydrogel becomes smooth. Atomic force microscopic (AFM) images further confirm this observation. The pristine PVA hydrogel shows a roughness of 61.9 nm while the roughness in PVA/KOH and PVA/KI samples is 2.8 nm and 1.0 nm (Supplementary Fig. 13), respectively. This indicates that the ions can reduce the inter-molecular interaction between polymer chains.

Such a change in interaction is quantified by measuring the viscosity of these hydrogels (Fig. 2c). The viscosity follows a

A/KCl (231 mPa·s) < PVA/KNO3 (235 mPa·s) < PVA/KOH (246

mPa·s) < pristine PVA (308 mPa·s). This implies that interaction among PVA chains is weakened with the addition of the potassium compounds, and different anions exhibits various degrees of weakening effect.

Fourier transform infrared spectroscopy (FT-IR) also confirmed this observation. The absorption peak within 3200–3600 cm^{-1} relates to hydroxyl stretching mode[30]. Figure 2d shows the peak intensity of this mode in PVA/KI hydrogel is higher than that of the pristine and PVA/KOH hydrogels, indicating that more hydroxyl groups can stretch in PVA/KI hydrogels than in other two samples. Moreover, the absorption peak of PVA/KI is blue-shifted compared with pristine and PVA/KOH hydrogels, indicating weaker hydrogen bonding[31]. This further proves ions can break the hydrogen bonds among PVA chains, with I^- ions exhibiting stronger ability for hydrogen bond breaking than OH^- ions.

A measurement of the water retention ability (see Note 3 in Supplementary Information) of the salt-incorporated hydrogels (Fig. 2e and Supplementary Fig. 14) reveals PVA/KI hydrogel retained the highest water content after 210 min. This suggests I^- ions liberate more hydroxyl groups that can hold more water molecules, resulting in slower water evaporation.

According to Y. Marcus et al., a water molecule forms 1.55 hydrogen bonds on average with surrounding molecules at room temperature[32]. The standard molar Gibbs free energy of transfer ΔG_{HB} characterizes changes in local water structure (hydrogen bonding network) when perturbed by a solute ion[32–35]. A more positive (negative) ΔG_{HB} value signifies a greater degree of promotion (destruction) of hydrogen bonds. All five anions used in this study exhibit a negative ΔG_{HB} (Fig. 2e), meaning they are all structure breakers[33]. More specifically, the absolute ΔG_{HB} value of the five anions follows a trend of - $OH^- < NO_3^- \approx Cl^- < Br^- < I^-$. This trend is consistent with the above-mentioned results on TE performance and structural analyses.

Based on these results, a physical model is proposed to explain the ion-polymer interaction on the thermoelectric performance of our i-TE materials. As mentioned, ionic thermal voltage stems from the Soret effect (Fig. 3a). The Seebeck coefficient obtainable by the thermal diffusion of ions with dissimilar mobilities can be expressed as[4,22]:

$$S_{td} = \frac{D_+ \hat{S}_+ - D_- \hat{S}_-}{e\left(D_+ + D_-\right)} \#(1)$$

where the subscript + (-) represents a cation (anion), e is the elementary charge, D and $\hat{S}$ are the mass diffusion coefficient and the Eastman entropy of transfer, respectively. Eq. (1) indicates the greater the difference between the mass diffusion coefficient or Eastman entropy of transfer of the cations and anions, the larger Seebeck coefficient is obtainable.

The dissolved ions in water can influence the nature of hydrogen bonds in their vicinity, i.e. either increasing (kosmotropic effect) or destroying (chaotropic effect) the local order around these ions[4,6,36]. If an ion promotes (disrupts) the order of the surrounding bonding network, it is called a structure maker (breaker)[33,37,38]. The degree of disruption of hydrogen bonding network varies for ions with different ΔG_{HB} values, leading to different hydration shell structures[39] (as sketched in Fig. 3b and 3c).

The different hydration shell structures caused by structure breakers have a direct impact on the whole hydrogel system. The structure breaker can disrupt the hydrogen bonds formed by the hydroxyl groups between adjacent PVA chain segments, in addition to the hydrogen bonds between water and structure breaker. On one hand, hydroxyl groups from disrupted hydrogen bonds are exposed to form stronger interaction with ions or H_2O[40]. On the other hand, the disruption of the hydrogen bonds among water molecules will thin the hydration shell of ions, making ions more exposed and interacting more strongly with the hydroxyl group (as shown in Fig. 3e). Conversely, if the structure maker ion promotes the formation of hydrogen bonds, the ion will promote the cross-linking between polymers, as sketched in Fig. 3d. These two effects will ultimately slow down the movement of anions with structure breaker characteristics.

Different from anions, the chaotropic effect of cations is not obvious[41]. The electronegativity of the cation determines the binding strength between the cation and the polar groups on the polymer chains, and thus affects the thermal diffusion rate of the cations. Besides the above-mentioned ion-polymer interactions, we do not exclude possible contribution from water evaporation that occurs for all hydrogels.

Because ions cannot flow through external circuits, ionic thermoelectric generators convert heat to electricity conversion in the form of capacitors[3,23]. Details regarding capacitance performance test can be found in the Supplementary Information. Figure 4a shows the four operation stages of an ionic thermoelectric capacitor[3,8,17,42]. First, the voltage increases during charging process under a temperature gradient (Stage I). Then, the charge accumulated on the electrode is released to the external circuit to do work when a load is connected (Stage II). Upon removal of the temperature difference and the external circuit is disconnected, the ions diffuse back to their initial state (Stage III). Finally, the external circuit is closed and the accumulated charges on the electrode flow through the load again (Stage IV).

The stage II time discharge curves and power density as a function of external load resistance are shown in Figs. 4b and 4c. The power density profile exhibits a parabolic relationship, with a maximum reaching1.31 J m^{-2} when the external load is 68 kΩ. The large power density generated under such a small temperature difference verifies the superior thermoelectric performance of our hydrogel.

It should be noted that the thickness of the hydrogel has a huge effect on the charging time and discharge power density, but does not affect its Seebeck coefficient. For example, the discharge time for a 300 μm PVA/NaI hydrogel is 1600 s, while that of a thicker (1000 μm) sample is 10000 s (Supplementary Fig. 16). The increase in charging time brings about simultaneous increase in power density (from 0.34 to 1.25 J m^{-2}) (Supplementary Fig. 17) due to an increased amount of charges stored in the gel network. Thus, a longer charging time leads to an increase in power density.

The quasi-continuous operation mode of the ionic thermoelectric capacitor is evaluated. After charging for ~ 1800 s under a temperature difference of ~ 1.4 K, the device reaches a saturation voltage of ~ 60 mV (Fig. 4d). Afterwards, the capacitor is connected to an external circuit with a load of 1 kΩ and discharged to almost 0 V in 1 ~ 3 s. Then it is recharged to its original voltage within 3 ~ 5 s (Fig. 4e and Supplementary Video 1). This charging rate is faster than other reported ionic thermoelectric capacitors[22,27]. Our hydrogel can easily complete more than 100 charge/discharge cycles within ~ 600 s, showing good cycle stability (Fig. 4d).

Despite the good cyclability and fast charge/discharge rate, the hydrogels are transparent in the visible region. The transmittance is more than 94% in the wavelength range between 400 nm and 800 nm (Fig. 4f). Finally, we demonstrate that good adhesion of the PVA/NaI hydrogel makes it suitable for wearable electronics. The hydrogel on a flexible PET substrate retains its original shape and does not de-laminate even when subjected to repeated bending and distortion (Supplementary Fig. 18 and Supplementary Video 2).

In summary, we have developed a series of excellent ionic thermoelectric materials, which are based on PVA/alkali metal compound hydrogels. The mechanistic study shows that electronegativity of the cations and Gibbs free energy of transfer of the anions are two key factors in modulating the ion-polymer interaction in our material system. The Seebeck coefficient of the PVA/CsI hydrogel prepared in this work reaches a record of 52.9 mV K^{-1}. The PVA/NaI hydrogel exhibits both high Seebeck coefficient (42.8 mV K^{-1}) and good ionic conductivity (51.5 mS cm^{-1}), leading to a superior ZT value of 5.09. Transparent, flexible and robust ionic thermoelectric capacitors are demonstrated. We believe the high-performance ionic thermoelectric materials will play an important role in harvesting low-grade thermal energy.

References And Notes

1. Liu, X. et al. Power generation from ambient humidity using protein nanowires. *Nature* **578**, 550-554, doi:10.1038/s41586-020-2010-9 (2020).
2. L. E. Bell, Cooling, heating, generating power, and recovering waste heat with thermoelectric systems. *Science* **321**, 1457-1461. doi:10.1126/science.1158899 (2008).
3. Zhao, D. et al. Ionic thermoelectric supercapacitors. *Energy Environ. Sci.* **9**, 1450-1457, doi:10.1039/c6ee00121a (2016).
4. Bonetti, M., Nakamae, S., Roger, M. & Guenoun, P. Huge Seebeck coefficients in nonaqueous electrolytes. *J. Chem. Phys.* **134**, 114513, doi:10.1063/1.3561735 (2011).
5. Li, S. & Zhang, Q. Ionic Gelatin Thermoelectric Generators. *Joule* **4**, 1628-1629, doi:10.1016/j.joule.2020.07.020 (2020).
6. Zhao, D. et al. Polymer gels with tunable ionic Seebeck coefficient for ultra-sensitive printed thermopiles. *Nat. Commun.* **10**, 1093, doi:10.1038/s41467-019-08930-7 (2019).
7. Li, T. et al. Cellulose ionic conductors with high differential thermal voltage for low-grade heat harvesting. *Nat. Mater.* **18**, 608-613, doi:10.1038/s41563-019-0315-6 (2019).
8. Cheng, H., He, X., Fan, Z. & Ouyang, J. Flexible quasi-solid state ionogels with remarkable seebeck coefficient and high thermoelectric properties. *Adv. Energy Mater.* **9**, 1901085, doi:10.1002/aenm.201901085 (2019).
9. Shu, Y. et al. Cation effect of inorganic salts on ionic Seebeck coefficient. *Appl. Phys. Lett.* **118**, 103902, doi:10.1063/5.0043498 (2021).
10. Snyder, G. J. & Toberer, E. S. complex thermoelectric materials. *Nat. Mater.* **7**, 105-114 (2008).
11. Yao, H. et al. Recent Development of Thermoelectric Polymers and Composites. *Macromol Rapid Commun* **39**, 1700727, doi:10.1002/marc.201700727 (2018).
12. Russ, B., Glaudell, A., Urban, J. J., Chabinyc, M. L. & Segalman, R. A. Organic thermoelectric materials for energy harvesting and temperature control. *Nat. Rev. Mater.* **1**, 16050, doi:10.1038/natrevmats.2016.50 (2016).
13. Zhang, Q., Sun, Y., Xu, W. & Zhu, D. Organic thermoelectric materials: emerging green energy materials converting heat to electricity directly and efficiently. *Adv. Mater.* **26**, 6829-6851, doi:10.1002/adma.201305371 (2014).
14. Kim, B. et al. Robust high thermoelectric harvesting under a self-humidifying bilayer of metal organic framework and hydrogel layer. *Adv. Funct. Mater.* **29**, 1807549, doi:10.1002/adfm.201807549 (2019).
15. Liu, W., Qian, X., Han, C.-G., Li, Q. & Chen, G. Ionic thermoelectric materials for near ambient temperature energy harvesting. *Appl. Phys. Lett.* **118**, 020501, doi:10.1063/5.0032119 (2021).
16. Abraham, T. J., MacFarlane, D. R. & Pringle, J. M. Seebeck coefficients in ionic liquids–prospects for thermo-electrochemical cells. *Chem Commun (Camb)* **47**, 6260-6262, doi:10.1039/c1cc11501d (2011).
17. Akbar, Z. A., Jeon, J.-W. & Jang, S.-Y. Intrinsically self-healable, stretchable thermoelectric materials with a large ionic Seebeck effect. *Energy Environ. Sci.* **13**, 2915-2923, doi:10.1039/c9ee03861b (2020).
18. Jiang, Q. et al. High thermoelectric performance in n-Type perylene bisimide induced by the Soret effect. *Adv. Mater.* **32**, 2002752, doi:10.1002/adma.202002752 (2020).
19. He, M., Qiu, F. & Lin, Z. Towards high-performance polymer-based thermoelectric materials. *Energy Environ. Sci.* **6**, 1352-1361, doi:10.1039/c3ee24193a (2013).
20. Culebras, M., Gomez, C. M. & Cantarero, A. Review on Polymers for Thermoelectric Applications. *Materials* **7**, 6701-6732, doi:10.3390/ma7096701 (2014).
21. Pu, S. et al. Thermogalvanic hydrogel for synchronous evaporative cooling and low-grade heat energy harvesting. *Nano Lett.* **20**, 3791-3797, doi:10.1021/acs.nanolett.0c00800 (2020).
22. Han, C.-G. et al. Giant thermopower of ionic gelatin near room temperature. *Science* **368**, 1091-1097 (2020).
23. [illegible] *Science* **371**, 343-344, doi:10.1126/science.abf3342 (2021).

24. Würger, A. Thermal non-equilibrium transport in colloids. *Rep. Prog. Phys.* **73**, 126601, doi:10.1088/0034-4885/73/12/126601 (2010).
25. Dietzel, M. & Hardt, S. Thermoelectricity in Confined Liquid Electrolytes. *Phys. Rev. Lett.* **116**, 225901, doi:10.1103/PhysRevLett.116.225901 (2016).
26. He, X., Cheng, H., Yue, S. & Ouyang, J. Quasi-solid state nanoparticle/(ionic liquid) gels with significantly high ionic thermoelectric properties. *J. Mater. Chem. A* **8**, 10813-10821, doi:10.1039/d0ta04100a (2020).
27. Horike, S. et al. Outstanding electrode-dependent Seebeck coefficients in ionic hydrogels for thermally chargeable supercapacitor near room temperature. *ACS Appl. Mater. Interfaces* **12**, 43674-43683, doi:10.1021/acsami.0c11752 (2020).
28. Fang, Y. et al. Stretchable and transparent ionogels with high thermoelectric properties. *Adv. Funct. Mater.* **30**, 2004699, doi:10.1002/adfm.202004699 (2020).
29. Wang, C. et al. Contributed Review: Instruments for measuring Seebeck coefficient of thin film thermoelectric materials: A mini-review. *Rev Sci Instrum* **89**, 101501, doi:10.1063/1.5038406 (2018).
30. Mansur, H. S., Oréfice, R. L. & Mansur, A. A. P. Characterization of poly(vinyl alcohol)/poly(ethylene glycol) hydrogels and PVA-derived hybrids by small-angle X-ray scattering and FTIR spectroscopy. *Polymer* **45**, 7193-7202, doi:10.1016/j.polymer.2004.08.036 (2004).
31. Takouachet, R. et al. Structural analysis and IR-spectroscopy of a new anilinium hydrogenselenite hybrid compound: A subtle structural phase transition. *Inorganica Chimica Acta* **446**, 6-12, doi:10.1016/j.ica.2016.02.047 (2016).
32. Marcus, Y. & Ben-Naim, A. A study of the structure of water and its dependence on solutes, based on the isotope effects on solvation thermodynamics in water. *The Journal of Chemical Physics* **83**, 4744-4759, doi:10.1063/1.449000 (1985).
33. Marcus, Y. Viscosity B-Coefficients, Structural Entropies and Heat Capacities, and the Effects of Ions on the Structure of Water. *J. Solution Chem.* **23**, 831-848, doi:10.1007/BF00972677 (1994).
34. G. Hummer, S. Garde, A.E. Garc õ & Pratt, L. R. New perspectives on hydrophobic effects. *Chem. Phys.* **258**, 349-370 (2000).
35. H. Donald B. Jenkins & Marcus, Y. Viscosity B-coefficients of ions in solution. *Chem. Rev.* **95**, 2695-2724 (1995).
36. Collins, K. D. & Washabaugh, M. W. The Hofmeister effect and the behaviour of water at interfaces. *Q. Rev. Biophys.* **18**, 323-422, doi:10.1017/s0033583500005369 (1985).
37. Marcus, Y. Effect of ions on the structure of water-structure making and breaking. *Chem. Rev.* **109**, 1346–1370 (2009).
38. Ohtaki, H. & Radnai, T. Structure and dynamics of hydrated ions. *Chem. Rev.* **93**, 1157-1204, doi:10.1021/cr00019a014 (2002).
39. Huang, B. et al. Non-covalent interactions in electrochemical reactions and implications in clean energy applications. *Phys. Chem. Chem. Phys.* **20**, 15680-15686, doi:10.1039/c8cp02512f (2018).
40. Shi, Y. et al. Enhancement of the mechanical properties and thermostability of poly(vinyl alcohol) nanofibers by the incorporation of sodium chloride. *J. Appl. Polym. Sci.***135**, 45981, doi:10.1002/app.45981 (2018).
41. R. Mancinelli, A. Botti, F. Bruni & Ricci, M. A. Hydration of sodium, potassium, and chloride ions in solution and the concept of structure maker breaker. *J. Phys. Chem. B* **111**, 13570-13577 (2007).
42. Yao, B. et al. Ultrahigh-conductivity polymer hydrogels with arbitrary structures. *Adv. Mater.* **29**, 1700974, doi:10.1002/adma.201700974 (2017).

Methods

Preparation of i-TE hydrogels

The inorganic salt or alkali was dissolved in deionized water at a certain concentration and stirred for 30 min to obtain a well-dispersed electrolyte solution. The selected inorganic salts or alkalis are CsI, KI, NaI, KBr, KCl, KNO_3 and KOH, respectively. Flocculent PVA was then added to the solution and stirred at 110 ^oC to obtain the hydrogel. The mass ratio of PVA to deionized water is 1:7. As an example, the preparation of 1 M PVA/NaI hydrogel is as follows. Firstly, dissolving 0.21 g NaI in 1.4 g DI and stirring for 30 minutes to obtain the inorganic salt solution. Afterwards, 0.2 g of PVA was added, and stirred at 110 ^oC for about 45 min to obtain 1 M PVA/NaI hydrogel. The glass substrate (20 mm×20 mm) was cleaned with detergent, deionized water, acetone and isopropanol for 15 min, respectively, and then dried with nitrogen. Two electrodes (1 mm×20 mm) with a spacing of 2 mm were attached to the glass substrate.[43] In the case of silver electrodes, a silver paste suspension was drop-casted on a self-made template, annealed at 120 ^oC for 30 minutes and treated with UV-ozone for 5 min. For copper electrodes, double-sided conductive copper foil was pasted directly on the glass base. The i-TE hydrogel was then drop-casted on the glass substrate with an area of 20 mm×13 mm. The Seebeck coefficient of all samples were measured at the relative humidity of 50% ~ 70%.

Material characterization

For cyclic voltammetry (CV) scan, the hydrogels were filled in a cylindrical container with stainless steel electrodes, and the voltage window from -0.15 V to +0.38 V was measured by Bio-logic (Gamry biologic, America), in which one platinum sheet served as the working electrode while the other one served as the counter and reference electrodes simultaneously. The scan rate was 10 mV s^{-1}. The electrochemical impedance spectroscopy (EIS) (Gamry biologic, America) measurement is to investigate the resistance of the hydrogels between 0.1 Hz and 100 kHz at the AC amplitude of 10 mV. The thermal conductivity was measured with a thermal conductivity meter (TC3000L, Shanxi China). The ratio of PVA to water in the hydrogel was diluted to 1:17.5 to test the corresponding viscosity (BROOKFIELD-DV3T). The hydrogels were freeze-dried for 48 hours using SCIENTZ-10N for SEM measurement (TM4000Plus II, Hitachi LTD). For atomic force microscope (AFM) (MicroNano D-5A) measurement, the hydrogel samples was spin-coated on a 1.5□1.5 cm glass substrate, and then air dried under ambient conditions for 2 hours.

Ionic conductivity measurement

The ionic conductivity of the hydrogels was determined by the EIS. The hydrogels were filled in a cylindrical container with stainless steel electrodes leading from the top to the bottom to perform potentiostatic scanning with a voltage amplitude of 10 mV, and the frequency ranges from 0.1 Hz to 100 kHz. After the ionic resistance (R) is obtained, the conductivity can be calculated according to the following formula:

$$\sigma = \frac{1}{R}\frac{l}{A}$$

Where *l* and A is the distance and the area of the electrodes respectively. In this work, *l* is 2 mm and R is about 200 mm^2.

Data availability

All data that support the findings of this study are contained in the Article and its Supplementary Information; any further relevant data are available from corresponding authors upon reasonable request.

Methods references

43. S. v. Reenen et al., Correcting for contact geometry in Seebeck coefficient measurements of thin film devices. *Organic Electronics* 15, 2250-2255 (2014). doi:10.1016/j.orgel.2014.06.018

Declarations

Funding: This work was supported by the National Natural Science Foundation of China (62074022), Fundamental Research Funds for the Central Universities (2020CDJQY-A055) and the Key Laboratory of Low-Grade Energy Utilization Technologies and Systems (LLEUTS2019001). **Author contributions:** K.S. and Y.J.H. conceived the idea and supervised the project. Y.J.H and H.L.C conducted the experiment. Q.Z., Y.J.Z and B.Q. carried out the DFT calculation. Y.S., Y.L.Z., J.L., M.L. calibrate the test system. K.S., J.O., Y.J.H., H.L.C., Y.S., Y.L., Y.G., G.O.O. and S.S.C. analyzed the data. K.S., J.O., Y.J.H., Q.Z. and H.L.C. wrote the paper. All authors discussed the results and approved the final version of the manuscript.

Competing interests The authors declare no competing interests.

Supplementary Information is available for this paper.

Correspondence and requests for materials should be addressed to K.S.

Peer review information

Reprints and permissions information

Figures

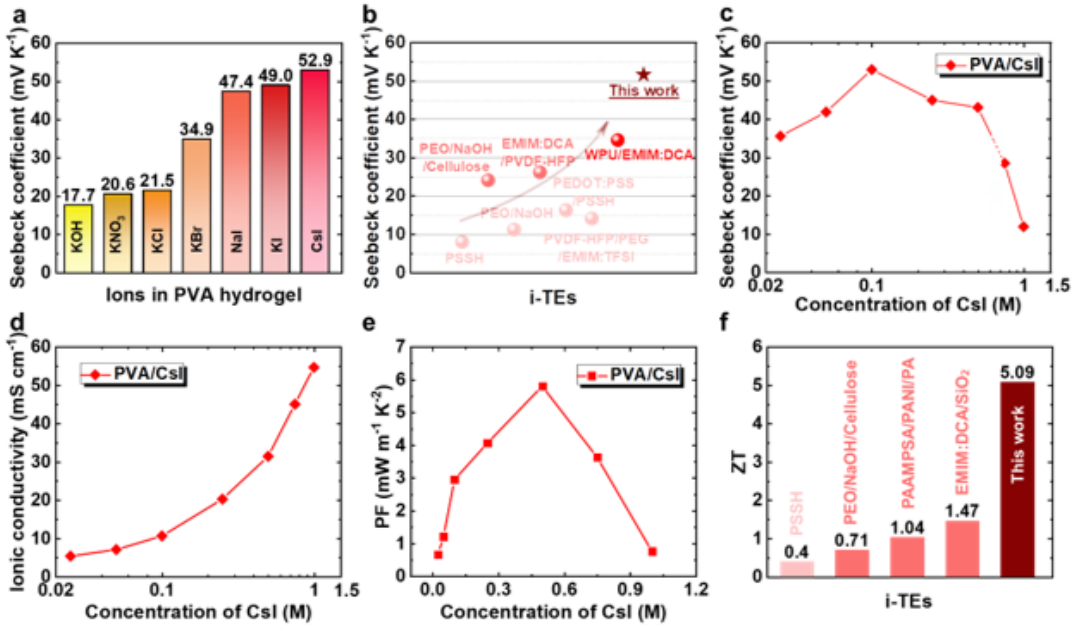

Figure 1

Thermoelectric properties of i-TE materials. a, The Seebeck coefficients of hydrogels with 0.1 M of various salts. b, A comparison of Seebeck coefficient of 0.1 M PVA/CsI hydrogel and other reported ionic thermoelectric materials. c, Seebeck coefficients of PVA/CsI hydrogel with different concentrations. d, The ionic conductivity of PVA/CsI hydrogel at different

concentrations. e, The power factor (PF) of PVA/CsI hydrogel at different concentrations. f, The ZT value of 1 M NaI hydrogel and other reported i-TE materials.

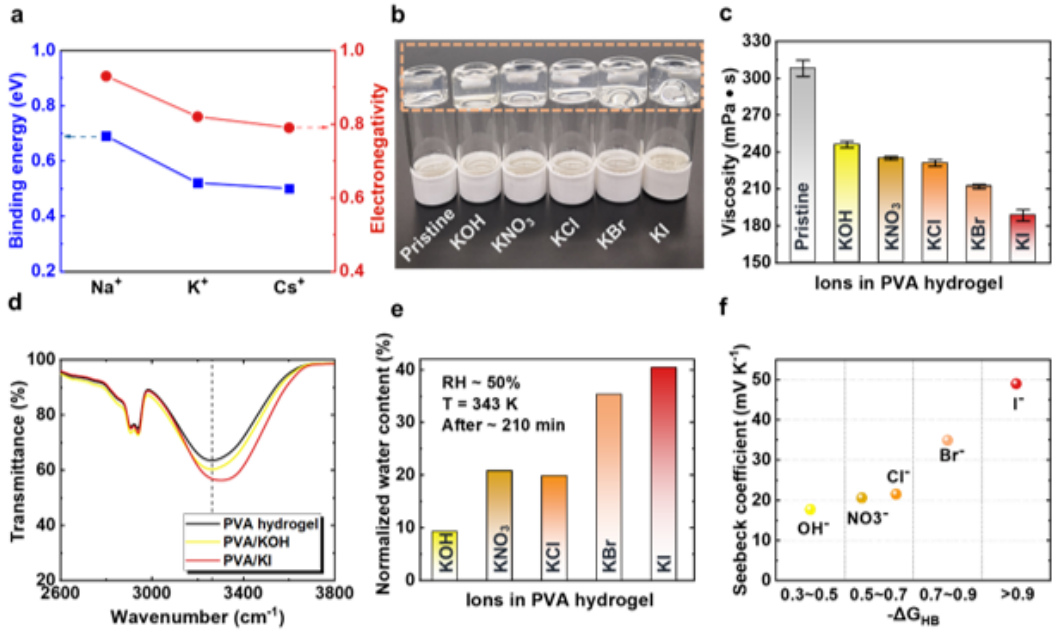

Figure 2

Phenomenon and characterization of the high i-TE properties. a, The binding energy of different alkali metal cations with the hydroxyl group on PVA and their electronegativity. b, Photographs of PVA/x hydrogel containing 0.1 M of x. (x = KI, KBr, KCl, KNO3, KOH and DI). A magnetic stirring pill is in the bottle. c, The viscosity of the diluted hydrogel. The mass ratio of PVA to DI is diluted to 1:17.5. The error bars (1 s.d. from five measured samples) were obtained from three measured samples with standard deviations of 6.4, 2.5, 1.3, 2.5, 1.6 and 4.4 mPa·s. d, Fourier infrared spectroscopy of the pristine PVA hydrogel, PVA/KOH and PVA/KI. e, Water retention properties of different hydrogel materials. All the hydrogel samples were simultaneously heated at 70 °C. f, The relationship between Seebeck coefficient and the –ΔGHB values of the anions.

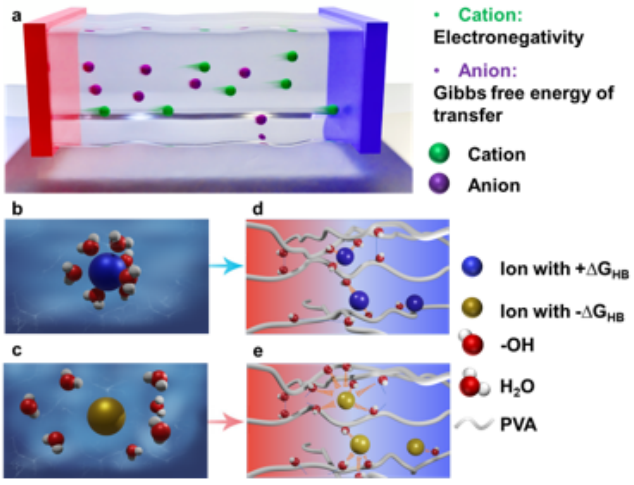

Figure 3

Thermal diffusion and migration model of ions with high i-TE properties. a, Schematic of ion thermal diffusion in hydrogel. b, Schematic of structure making ions (and the structure breaking ion in c) in aqueous solution. d, Structure making ion for

hydrogen bond disruption between PVA chains. e, Structure breaking ion for hydrogen bond disruption between PVA chains.

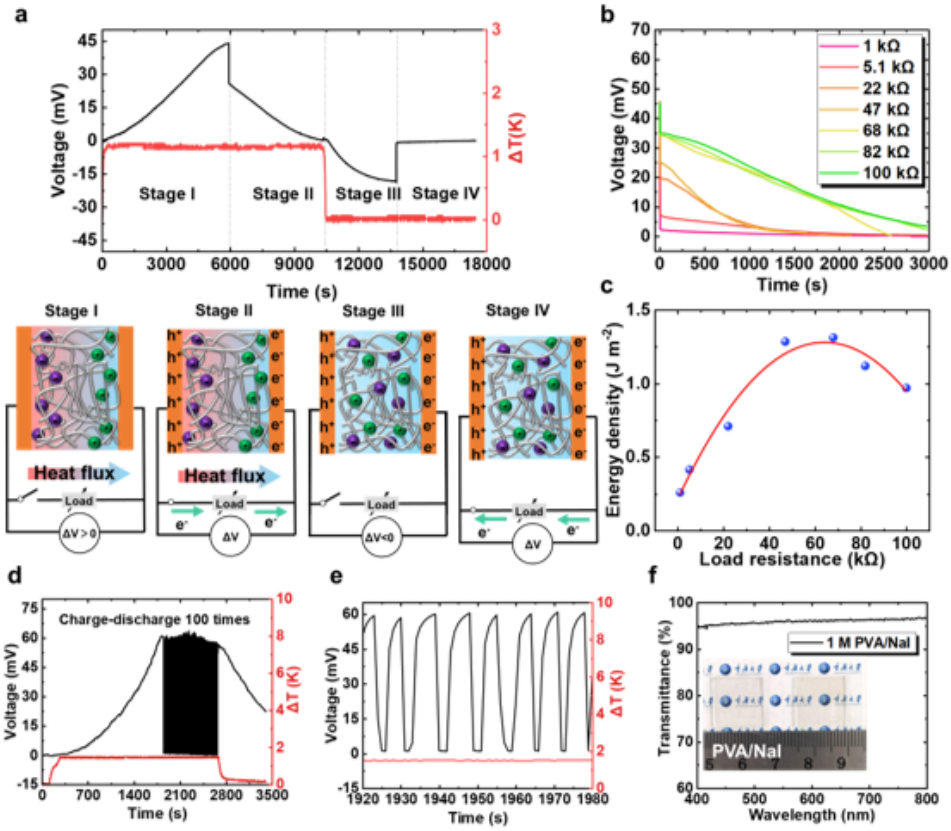

Figure 4

Operating characteristics and property of an i-TE supercapacitors. a, Voltage profile of PVA/NaI hydrogel using an external load of 47 kΩ. The concentration of the NaI is 1mol/L. The plot shows the corresponding four stages. b, The voltage curves and c energy density of the second stage at different external loads. All the hydrogel were heated at ~1.1 K and measured with Cu electrode. d, The quasi-continuous hot charge/discharge process of i-TE supercapacitor was carried out 100 times under the temperature difference of ~1.4K (Cu electrode). The concentration of NaI is 1M. e, Part of the charge/discharge process voltage curve. f, UV–vis transmittance spectra of a PVA/NaI hydrogel on the glass substrate. The illustration shows the PVA/NaI hydrogel on a glass substrate (left) and a pure glass substrate (right). The transmittance of the hydrogel was more than 94% in the visible light range.

Supplementary Files

This is a list of supplementary files associated with this preprint. Click to download.

- MovieS1ChargingDischargingofthePVANaIiTECapacitor.mp4
- MovieS2DemonstrationofMechanicalPropertiesofthePVANaIHydrogel.mp4
- SupplementaryinformationHydrogelswithGiganticThermopowerforLowgradeHeatHarvestingrevisedwithoutmarks.docx